Published in final edited form as:
Dev Cell. 2008 June ; 14(6): 914–925. doi:10.1016/j.devcel.2008.03.022.

Synaptotagmin VII Regulates Bone Remodeling by Modulating Osteoclast and Osteoblast Secretion

Haibo Zhao[1,*], **Yuji Ito**[1], **Jean Chappel**[1], **Norma W. Andrews**[2], **Steven L. Teitelbaum**[1], and **F. Patrick Ross**[1,*]

1*Department of Pathology and Immunology, Washington University School of Medicine, St. Louis, MO 63110*

2*Section of Microbial Pathogenesis, Yale University School of Medicine, New Haven, CT 06510*

SUMMARY

Maintenance of bone mass and integrity requires a tight balance between resorption by osteoclasts and formation by osteoblasts. Exocytosis of functional proteins is a prerequisite for the activity of both cells. In the present study, we show that synaptotagmin VII, a calcium sensor protein that regulates exocytosis, is associated with lysosomes in osteoclasts and bone matrix protein-containing vesicles in osteoblasts. Absence of synaptotagmin VII inhibits cathepsin K secretion and formation of the ruffled border in osteoclasts and bone matrix protein deposition in osteoblasts, without affecting the differentiation of either cell. Reflecting these in vitro findings, synaptotagmin VII-deficient mice are osteopenic due to impaired bone resorption and formation. Therefore, synaptotagmin VII plays an important role in bone remodeling and homeostasis by modulating secretory pathways functionally important in osteoclasts and osteoblasts.

INTRODUCTION

The skeleton is a dynamic organ that undergoes continuous renewal by the physiological process of remodeling, in which bone resorption by osteoclasts precedes formation by osteoblasts. A tight balance between these two processes is required to maintain bone mass and integrity. In fact, most acquired systemic bone diseases of man are due to aberrant remodeling. Typically, enhanced osteoclastic bone resorption leads to a reduction of bone mass and compromised bone strength, which predisposes to an increased risk of fractures, as occurs in osteoporosis (Raisz, 2005; Zaidi, 2007). Alternatively, defects in osteoclast differentiation or function can result in an abnormal accumulation of bone, which may be structurally compromised, as observed in osteopetrosis and osteosclerosis (Tolar et al., 2004).

Osteoclasts are multinucleated cells formed by fusion of mononuclear precursors of the monocyte/macrophage lineage. Macrophage colony-stimulating factor (M-CSF) and receptor activator of nuclear factor kappa B (RANK) ligand (RANKL), the two principal osteoclastogenic cytokines, induce osteoclast precursors to express functionally important proteins which endow the cells with an efficient and unique machinery to resorb bone (Teitelbaum and Ross, 2003). In the process of matrix degradation attachment of osteoclasts to bone induces dramatic cytoskeleton reorganization, resulting in formation of a filamentous

*Correspondence: H.Z. (E-mail: hzhao@wustl.edu) or F.P.R. (E-mail: rossf@wustl.edu), Tel: (314) 454-8463, Fax: (314) 454-5505.

actin ring or sealing zone. This structure surrounds a specialized plasma membrane domain, the ruffled border, thus forming an isolated resorptive microenvironment between the osteoclast and underlying bone matrix. The ruffled border is generated by the fusion of secretory vesicles with the bone-apposing plasma membrane (Baron et al., 1988). During this process, protons and lysosomal enzymes, principally cathepsin K, are secreted vectorially into the resorption lacuna to dissolve bone mineral and digest organic matrix, respectively (Vaananen et al., 2000). However, the molecules modulating the transport and fusion of secretory vesicles with the plasma membrane have not been identified.

Osteoblasts arise from mesenchymal stem cells that can differentiate into fibroblasts, myoblasts, osteoblasts or adipocytes. The path from multipotent stem cells to osteoblasts is controlled by two key osteogenic transcription factors, Runx2 and osterix (Ducy et al., 2000). Mature osteoblasts synthesize and secrete type I collagen, noncollagenous proteins, enzymes and growth factors, which comprise major components of the organic matrix of bone (Harada and Rodan, 2003). This newly deposited bone matrix (osteoid) undergoes mineralization mediated by matrix vesicles, which are membrane-bound extracellular structures also secreted by osteoblasts (Anderson, 1995). In contrast to recent insights into transcriptional regulation of osteoblast differentiation, the secretory pathways and their mediators in osteoblasts remain largely unknown.

Exocytosis is a fundamental process through which eukaryotic cells release hydrophilic secretory products into the extracellular space, or translocate specific functional proteins to the plasma membrane (Chieregatti and Meldolesi, 2005; Verhage and Toonen, 2007). While the two major types of exocytosis, namely constitutive and regulated, differ in their regulatory mechanisms, fusion of exocytotic vesicles with the plasma membrane is the common final step in both intracellular membrane fusion, and is mediated by v- (vesicular) and t- (target) SNAREs (soluble N-ethylmaleimide-sensitive fusion protein (NSF) attachment protein (SNAP) receptors) (Jahn and Scheller, 2006). These proteins assemble to form a four-helix bundle juxtaposing vesicle and target membranes. Although SNAREs are sufficient to catalyze membrane fusion, additional proteins are required to achieve specificity and spatio-temporal control. Among these other regulators of membrane fusion is the synaptotagmin (Syt) family of vesicular trafficking proteins (Meldolesi and Chieregatti, 2004; Rizo et al., 2006).

Fifteen Syt isoforms have been identified in mammalian cells. Each Syt family member is distributed distinctly and exhibits different calcium- and phospholipid-binding affinities. While Syt I, II, III, V and X are expressed predominantly in the nervous system and neuro-endocrine cells, others are ubiquitous (Chapman, 2002; Sudhof and Rizo, 1996). In vitro biochemical and in vivo genetic studies implicate Syt I, the best characterized isoform, as an essential calcium sensor for fast, synchronous neurotransmitter release in neurons (Geppert et al., 1994). Unlike Syt I, which is localized largely on the membrane of synaptic vesicles, Syt VII is expressed broadly (Andrews and Chakrabarti, 2005). This isoform regulates calcium-dependent exocytosis of lysosomes in fibroblasts (Martinez et al., 2000) and neurons (Arantes and Andrews, 2006), dense-core vesicles in neuro-endocrine PC12 cells (Tsuboi and Fukuda, 2007; Wang et al., 2005), insulin containing secretory granules in pancreatic islet β-cells (Gao et al., 2000; Gauthier et al., 2007; Li et al., 2007), lytic granules/secretory lysosomes in cytotoxic lymphocytes (Fowler et al., 2007) and lysosome membrane delivery to phagosomes in macrophages (Czibener et al., 2006). Given that macrophages are osteoclast precursors and osteoblasts are specialized fibroblasts, Syt VII is a candidate to regulate calcium-dependent secretory activities in both cell types.

RESULTS

Syt VII regulates osteoclast lysosomal exocytosis and ruffled border formation

Like wild-type (WT) cells, Syt VII$^{-/-}$ osteoclasts cultured on bone slices formed characteristic actin-rings (Figure 1A), suggesting that cytoskeleton organization and the signals that activate this process are intact. However, the number of osteoclasts secreting cathepsin K into the resorption lacuna, shown by dual staining of the acidic collagenase and F-actin, was greatly reduced in the absence of Syt VII (Figure 1B and 1C). While the resorption pits in WT cultures were well-demarcated, those in Syt VII$^{-/-}$ osteoclast cultures were small and irregular (Figure 1D), reminiscent of those produced in the absence of the integrin αvβ3 (Feng et al., 2001). Consistent with these morphologic findings, CTx-I, the type-I collagen fragments cleaved by cathepsin K during bone resorption, was decreased in Syt VII$^{-/-}$ culture medium (Figure 1E). Therefore, despite their capacity to form actin rings, SytVII$^{-/-}$ osteoclasts have diminished bone resorptive capacity.

The ruffled membrane, the resorptive organelle of the osteoclast, is formed by insertion of lysosomes containing cathepsin K into the bone-apposed plasmalemma (Zhao and Vaananen, 2006). Consistent with arrested cathepsin K secretion, ruffled membranes which were apparent in WT cells (white arrows in the upper panel of Figure 1F) were absent in Syt VII$^{-/-}$ osteoclasts (Figure 1F, lower panel). The data above indicate that Syt VII regulates osteoclast function by modulating secretion of lysosomes containing cathepsin K, the major matrix-degrading hydrolase (Drake et al., 1996). Consistent with this conclusion, SytVII localized in perinuclear lysosomes with LAMP2, a lysosomal membrane protein, in cells cultured on plastic (Figure S1, see supplementary data available with this article online, upper panels). In resorbing osteoclasts cultured on bone Syt VII also associated with LAMP2, but in this circumstance both molecules were principally in the ruffled border (Figure S1, lower panels) which was circumscribed by actin rings (Figure 2A, upper panels). Moreover, Syt VII co-localized with cathepsin K (Figure 2B, upper panels).

Next, we fractionated the cytosol of mature osteoclasts by self-generated iodixanol density gradient ultracentrifugation. We collected 20 fractions and determined protein distribution by western blotting. As shown in Figure 2C, the peak of active cathepsin K (the 27kDa species) was located in the lysosomal fraction (fraction 2), identified by its LAMP-2 content, whereas the 36kD pro-form of the enzyme co-migrated with the trans-Golgi network marker syntaxin 6. Of relevance, Syt VII, Rab7 and TI-VAMP, all lysosomal proteins, were in fraction 2, which also had sec6 and sec8 (Figure 2D), two subunits of the exocyst, a conserved protein complex involved in the docking of exocytic vesicles at the plasma membrane (Boyd et al., 2004; TerBush et al., 1996). Thus, fraction 2 is enriched in proteins that are likely to be present in osteoclast secretory vesicles. Lastly, Syt VII and TI-VAMP, the lysosomal v-SNARE, formed a complex in osteoclasts (Figure 2E).

We also examined osteoclastogenesis. WT and SytVII$^{-/-}$ osteoclast precursors, in the form of bone marrow macrophages (BMMs), were cultured with RANKL and M-CSF. After 3 and 5 days, the cells were stained for TRAP activity as a marker of osteoclast differentiation. Expression of several osteoclast differentiation genes was also detected by RT-PCR and western blots at each stage. The total number of multinucleated TRAP^{+} osteoclasts, and levels of cathepsin K, MMP-9, β3 integrin mRNA and c-src and cathepsin K protein (Figure S2), were indistinguishable in WT and Syt VII$^{-/-}$ cells as they underwent osteoclastogenesis. Thus, Syt VII does not regulate osteoclast differentiation.

Syt VII regulates bone matrix protein secretion and nodule formation by osteoblasts

Osteoblasts derive from mesenchymal stem cells, as do fibroblasts, in which Syt VII regulates lysosome exocytosis (Martinez et al., 2000). To determine whether Syt VII deficiency has intrinsic effects on their differentiation and/or function, we isolated calvarial primary osteoblasts from new-born WT and Syt VII$^{-/-}$ mice and cultured them with time in differentiation medium. The number of alkaline phosphatase (ALP) expressing cells in WT and Syt VII$^{-/-}$ cultures was comparable (Figure 3A, 3B left panel), as was expression of osteocalcin, a marker of differentiated osteoblasts (Figure 3B, middle panel). In contrast, nodule formation in Syt VII null osteoblast cultures was decreased (Figure 3C). Next, we examined the secretion of type I collagen, a dominant bone matrix protein in WT and Syt VII$^{-/-}$ osteoblast cultures. Type I collagen is initially synthesized as a larger precursor, procollagen, with NH_2– and COOH-terminal propeptides that are released extracellularly by limited proteolysis (Prockop and Kivirikko, 1995). Thus, the level of intracellular pro-forms of type I collagen alpha chains in total cell lysates (Figure 3D) and extracellular mature alpha chains in pepsin-digested extracts (Figure 3E) was detected by western blots with the same anti-type I collagen antibody. The amount of type I collagen secreted into the extracellular matrix, as reflected by the ratio between pro- and mature forms of collagen alpha chains, was significantly decreased in Syt VII$^{-/-}$ osteoblasts compared to WT cells. Collectively, these data suggest that Syt VII regulates collagen secretion by osteoblasts rather than their differentiation.

We examined next the localization of Syt VII in osteoblasts, with particular focus on its association with secreted bone matrix proteins. Thus, freshly isolated calvarial primary osteoblasts were transduced with a retroviral vector containing Syt VII-GFP and selected with puromycin for 3 days. The cells were then re-plated and cultured on glass coverslips in osteoblast differentiation medium, and the distribution of Syt VII-GFP was detected by fluorescent microscopy. Syt VII-GFP was initially localized at perinuclear punctuate structures (Figure 4A, left panel). During osteoblast maturation, localization of these Syt VII-GFP positive vesicles changed from perinuclear to nodular (Figure 4A, right panels). These nodules also contained osteopontin (OPN) and osteocalcin (OC) (Figure 4B and 4C). To characterize further the subcellular localization of Syt VII in osteoblasts, we used the same self-generated iodixanol density gradient ultracentrifugation applied to osteoclasts to fractionate the cytosol of mature osteoblasts. Syt VII was found in a dense fraction that again contained sec6 and sec8, but lacked the Golgi marker, syntaxin 6 (Figure 4D). Importantly, several bone matrix proteins including type I collagen, osteocalcin, osteopontin are enriched in the same fraction (Figure 4E). Together with the co-localization and functional studies shown above in Figure 4A–C and Figure 3C–D, respectively, these data establish that matrix secretion in osteoblasts is regulated by Syt VII.

Retroviral transduction of WT Syt VII rescues the phenotypes of Syt VII$^{-/-}$ osteoclasts and osteoblasts

To confirm that Syt VII regulates cell autonomous effects in osteoclasts and osteoblasts, we constructed a retroviral vector expressing Syt VII. Transduction of the recombinant virus into SytVII$^{-/-}$ osteoclast precursors rescued osteoclastic bone resorption completely, as demonstrated by cathepsin K secretion (Figure 5A), pit formation (Figure 5B), and medium CTx-I levels (Figure 5C). Similarly, retroviral transduction of SytVII$^{-/-}$ osteoblasts restored their capacity to generate bone nodules (Figure 5D) which is probably due to enhanced type I collagen secretion into extracellular matrix in Syt VII but not in empty vector transduced osteoblasts (Figure 5E and 5F).

Syt VII$^{-/-}$ mice are osteopenic due to decreased bone resorption and bone formation

Secretion is a key step for both osteoclastic bone resorption and osteoblastic bone formation, indicating that Syt VII may regulate bone remodeling in vivo. To test this hypothesis, we characterized the bone phenotype of Syt VII$^{-/-}$ mice. Micro-computed tomography (μCT) analysis of the distal femora from 2-month old WT and Syt VII$^{-/-}$ mice revealed that the null mice had a dramatic decrease in trabecular bone volume (Figure 6A and 6B). Consistent with this finding, Syt VII$^{-/-}$ mice had decreased trabecular thickness and increased trabecular separation (Figure 6C–6D). Bone mineral density was also significantly lower in Syt VII$^{-/-}$ mice than in WT mice (Figure 6E). Serum levels of CTx-I (Figure 7A) and osteocalcin (Figure 7B), global biomarkers of bone resorption and bone formation respectively, were decreased in knockout animals. Overall, these data indicate that the observed lower bone mass in Syt VII$^{-/-}$ mice results from decreased remodeling. In keeping with this hypothesis, the amount of osteoid, unmineralized bone matrix newly deposited by osteoblasts, was significantly decreased in Syt VII$^{-/-}$ mice (Figure 7C) despite normal numbers of osteoclasts and osteoblasts (Figure 7D and 7E). Moreover, when compared to WT controls, the results of double calcein labeling in Syt VII$^{-/-}$ mice showed an almost three-fold decrease in mineral apposition and total bone formation rates (Figure 7F–7H). Additionally, the level of circulating PTH, a key bone remodeling regulating hormone, is similar in WT and Syt VII mutant mice (Figure 7I and 7J), indicating that there is no overt dysfunction of the parathyroid glands or kidneys. Taken together with previous report that there are no histological abnormalities in major organs such as brain, liver, heart, exocrine pancreas, spleen and kidneys (Chakrabarti et al., 2003), we conclude that the skeletal phenotype observed in this study results from cell autonomous defects in osteoclasts and osteoblasts. Finally, mice lacking synaptotagmin VII exhibit no abnormalities in skeletal patterning (data not shown), suggesting that the protein plays no role in modeling of bone. In contrast, it clearly is important in postnatal bone remodeling, as shown by development of osteopenia in adult animals.

DISCUSSION

The exocytosis of functional proteins is a prerequisite for osteoclast and osteoblast function. In the context of osteoclasts, the cells secrete hydrochloric acid to dissolve bone salts, a process that is mediated by a vacuolar-type proton pump and charge-coupled chloride channel, and release the lysosomal acidic hydrolase cathepsin K to digest the organic matrix of bone. Recent genetic studies in humans and rodents have unveiled several essential components of the osteoclast resorptive machinery, including the a3 subunit of vacuolar type proton pumps (Frattini et al., 2000; Li et al., 1999), ClC-7 chloride channel (Kornak et al., 2001), OSTM1 (also called grey lethal and recently identified as the β subunit/chaperone of ClC-7) (Chalhoub et al., 2003; Lange et al., 2006), and cathepsin K (Gelb et al., 1996; Saftig et al., 1998). Interestingly, these pumps, channels and hydrolases are enriched in endocytic compartments in most cell types, especially lysosomes (Schroder et al., 2007) and in inactive non-resorbing osteoclasts. These proteins translocate to the ruffled border or are secreted into the resorption lacuna during bone resorption (Lange et al., 2006; Zhao and Vaananen, 2006). Therefore, one of the mechanisms by which they can be targeted to the ruffled border is through regulated lysosomal exocytosis (Baron et al., 1988). If this is the case, one would expect that the molecules regulating the trafficking and/or the fusion of lysosomes with the plasma membrane are also critical for osteoclast function. Consistent with this notion, inhibition of the expression of Rab7, a small GTPase that specifically regulates late endosomal/lysosomal vesicular trafficking, impairs osteoclast secretion and ruffled border formation (Zhao et al., 2001). In the current study, we identified Syt VII as a key molecule regulating the fusion of lysosomes with the ruffled border membrane and showed that it is important for osteoclast function.

Syt VII, a ubiquitously expressed and evolutionarily conserved member of the Syt family, was first implicated in the regulation of lysosomal exocytosis and repair of plasma membrane wounding in fibroblasts (Martinez et al., 2000; Reddy et al., 2001). The function of Syt VII has recently been extended to the exocytosis of lysosomes and of some non-synaptic secretory granules in a range of specialized cells, including neuro-endocrine, chromaffin and pancreatic beta cells, as well as cytotoxic lymphocytes and macrophages (Czibener et al., 2006; Fowler et al., 2007; Gao et al., 2000; Gauthier et al., 2007; Li et al., 2007; Osborne et al., 2007; Tsuboi and Fukuda, 2007; Wang et al., 2005). Given an essential role of the lysosomal pathway for regulated secretion by osteoclasts, which are derived from macrophages, we postulated that Syt VII regulates bone resorption. We demonstrated in this study that genetic deletion of Syt VII inhibits but does not ablate completely cathepsin K secretion and formation of the ruffled border in osteoclasts. Earlier work in fibroblasts has shown that absence of Syt VII reduces lysosomal exocytosis by about 50%, but does not completely eliminate the process (Chakrabarti et al., 2003). This result may be because there is functional redundancy, with other calcium sensors partially compensating for the absence of Syt VII (Hammarlund et al., 2008; Rizo and Sudhof, 1998). The identity of these calcium binding proteins in osteoclasts remains unclear. Next, we showed Syt VII is a lysosomal protein in osteoclasts, a finding similar to that for other cell types. Syt VII co-localizes with Cathepsin K and LAMP2 on lysosomes and in a lysosome-enriched fraction containing Rab7 and sec6/sec8, two components of the exocyst complex mediating vesicular secretion (Boyd et al., 2004; TerBush et al., 1996). Syt VII, cathepsin K, LAMP2 and rab7 all translocate to the ruffled membrane in resorbing osteoclasts as do sec6/sec8 (Zhao H and Ross FP unpublished data). We also showed that Syt VII interacts with the lysosome-specific v-SNARE TI-VAMP, as previously reported in other cell types (Rao et al., 2004). A likely binding partner of the SytVII/TI-VAMP complex at the plasma membrane is syntaxin 4, a plasma membrane t-SNARE protein which recognizes Syt VII in other cells and is at the ruffled membrane in resorbing osteoclasts (Toyomura et al., 2003). Taken together, these data indicate that Syt VII promotes the fusion of lysosomes containing proton pumps, chloride channels and acidic hydrolases with the ruffled membrane, a step which is rate-limiting in bone resorption.

At least two types of secretory activities mediate bone formation by osteoblasts. The first is deposition of bone matrix proteins and the second is the delivery of matrix vesicles into the extracellular space to facilitate mineralization. The identity of these two sets of osteoblastic secretory vesicles is not clear, when compared to those of the osteoclast. In this study, we show for the first time, to our knowledge, that Syt VII specifically regulates secretion of bone matrix proteins such as type I collagen, thereby promoting bone nodule formation by osteoblasts without affecting their differentiation. Furthermore, Syt VII co-localized with osteocalcin and osteopontin at bone nodules and in a membrane fraction which also contains these proteins as well as type I collagen, and sec6/sec8. These data are consistent with the recent proteomic identification of Syt VII as a bone nodule protein (Gorski et al., 2005). The exact mechanism of Syt VII action in osteoblasts is not clear. It is possible that Syt VII, as in osteoclasts, mediates the fusion of matrix vesicles with plasma membrane through interaction with SNARE proteins and plasma membrane phospholipids (Prele et al., 2003). Another possibility is that osteoblasts use lysosomes as membrane suppliers for matrix protein secretion. A homologous process is used to repair plasma membrane damage via SytVII-regulated lysosome exocytosis in fibroblasts (Martinez et al., 2000; Reddy et al., 2001), cell that are related to osteoblasts.

A separate extracellular compartment is the matrix vesicle, identified and characterized by several groups including Anderson and colleagues (Anderson, 1995; Anderson et al., 2005; Wiesmann et al., 2005). These membrane-encapsulated structures are small (50–200 nm) and hence detectable only by electron microscopy, but play a unique and important role in calcification of newly deposited matrix of bone, cartilage or dentin (Garimella et al., 2004; Genge et al., 2003; Kirsch et al., 1997; Roberts et al., 2007; Takano et al., 2000). While most

data concerning matrix calcification are based on studies in bone and related tissues, new evidence shows that analogous vesicular structures have an important role in calcification of medial arteries (reviewed in (Shao et al., 2006)). Finally, a recent report describes a proteomic approach to examine the protein composition of highly purified matrix vesicles isolated from calcifying murine osteoblasts (Xiao et al., 2007). Of importance, a number of proteins known to be present in osteoid are absent in the matrix vesicle proteome, including type1 collagen, osteopontin and osteocalcin, all of which we find are readily detectable in our purified osteoblast fraction containing Syt VII. Thus, we conclude that our investigations have targeted not the matrix vesicle, but rather an intracellular compartment involved in secretion of proteins that comprise the major organic components of hard tissues.

Our finding that SytVII plays a similar functional role in osteoblasts and osteoclasts, the two cell types that regulate bone tissue, highlights the importance of calcium-regulated secretion in this system. As the multiple mammalian synaptotagmin isoforms emerged, a critical issue became the sub-cellular localization of each Syt member. Although this information is still not available for all Syt isoforms, only Syt VII has been consistently localized on lysosomes, and in some non-synaptic secretory vesicles of specialized cells (Andrews and Chakrabarti, 2005). Several other synaptotagmin isoforms are expressed in osteoclasts and osteoblasts but their levels do not change in the absence of Syt VII, except for a modest increase in Syt VI expression in mature osteoclasts compared to WT cells (Figure S3). Since the only known role for Syt VI is participation in the acrosome reaction in sperm (Michaut M et al, 2001; Hutt DM, et al., 2005) and the protein lacks the Ca^{2+}-dependent binding of SNAREs and phospholipids (Li C et al., 1995) we conclude that functional redundancy of other synaptotagmin isoforms in lysosomal secretion in osteoclasts and type I collagen secretion in osteoblasts is unlikely. In addition to the differential localization, the significantly different Ca^{2+} affinities of different Syt isoforms also suggest specialized activities. In this regard, Syt VII has a high calcium-binding affinity relative to Syt I (Sugita et al., 2002), which is a key regulator of neuronal synaptic vesicle exocytosis but is not expressed in osteoclasts. Thus, the phenotypes we detected for osteoclast and osteoblast function in Syt VII-deficient mice suggest that the secretory vesicles involved in bone remodeling in these two cell types may exocytose in response to relatively low (μM) cytosolic calcium elevations.

Since Syt $VII^{-/-}$ mice have the gene deleted in all tissues, we cannot rule out the possibility that systemic secretion defects in other organs or systems have effects on bone remodeling. However, our detailed cellular and biochemical studies in both osteoclasts and osteoblasts in vitro show that Syt $VII^{-/-}$ mice have intrinsic defects in the function of both cell types, leading to osteopenia caused by lower bone formation and resorption rates in Syt $VII^{-/-}$ mice. Moreover, earlier histology examination of major organs in Syt $VII^{-/-}$ mice (Chakrabarti et al., 2003) revealed that there are no abnormalities in organs such as brain, liver, heart, exocrine pancreas, spleen and parathyroid grands and kidneys. Additionally, the normal circulating PTH levels in Syt $VII^{-/-}$ mice reported in this study and the expected age-related changes in this parameter suggest that parathyroid gland function is normal. Finally, since changes in parathyroid secretion often reflect altered renal function, we deduce that the kidney is not impacted by loss of Syt VII.

Bone formation and resorption are two arms of a tightly coupled remodeling process. In post-menopausal women and ovariectomized animals, estrogen deficiency results in enhanced osteoclastogenesis and bone resorption, accompanied by increased bone formation. In each bone remodeling cycle, bone formation always lags behind resorption, prompting bone loss in this circumstance of high bone turnover. In contrast, patients with Type II or senile osteoporosis and SAMP6 and Runx2-II deficient mice have a decreased bone mass due to low bone turnover (Silva et al., 2004; Xiao et al., 2005). Thus, Syt $VII^{-/-}$ mice provide an animal model reflecting low turnover osteoporosis.

There are only a few examples in which a single protein suppresses the function of the two major cell types in bone. Karsenty and colleagues showed that in addition to its previously reported key role in osteoclast differentiation (Takayanagi et al., 2002), the transcription factor NFAT also modulates osteoblast proliferation and function (Winslow et al., 2006). Similarly, the Noda group reported recently that deletion of schnurri-2 results in osteopenia (Saita et al., 2007), by inhibiting differentiation of both osteoblasts and osteoclasts. More recently, disruption of AKT1, a serine/threonine kinase downstream of PI-3 kinase in mice has been shown to lead to low-turnover osteopenia via decreased differentiation and enhanced apoptosis in both osteoblasts and osteoclasts (Kawamura et al., 2007). In contrast, we find that the numbers of these two cell types are unaltered by absence of Syt VII, reinforcing the view that this protein acts by modulating secretion of a key matrix protease by osteoclasts and of bone matrix proteins by osteoblasts. Our findings provide one of the first molecular insights into the mechanism of regulated secretion by bone cells, a process that is central to their function and the regulation of bone mass.

EXPERIMENTAL PROCEDURES

Reagents and antibodies

Cell culture media were purchased from Sigma-Aldrich. Fetal bovine serum was purchased from Hyclone. Hoechst 33258 and peroxidase-conjugated wheat germ agglutinin were from Sigma-Aldrich. Alexa-488 and -546 conjugated phalloidins were bought from Invitrogen. Antibodies were obtained from the following sources: mouse anti-cathepsin K and rat anti-osteopontin monoclonal antibodies (Chemicon); rat anti-LAMP-2 monoclonal antibodies, ABL-93 and GL2A7, (Developmental Studies Hybridoma Bank, University of Iowa); rabbit anti-GFP polyclonal antibody (Invitrogen); mouse anti-syntaxin 6, anti-sec6 and anti-sec8 monoclonal antibodies (Stressgen); goat anti-Syt VII (N-18) and Rab7 (C19) antibodies (Santa Cruz); rabbit polyclonal anti-type I collagen antibodies (Calbiochem and Chemicon); mouse anti-osteocalcin antibody (Biomedical Technologies Inc). Mouse anti-TI-VAMP monoclonal antibody was a generous gift from Dr. T Galli (Institut National de la Sante et de la Recherche Medicale Avenir team, Paris, France). The fluorescein-labeled secondary antibodies used in immunofluorescence and western blots were purchased from Jackson ImmunoResearch Laboratories and Rockland, respectively.

Mice

The generation of Syt $VII^{-/-}$ mice has been reported previously (Chakrabarti et al., 2003). The mice were backcrossed to C57BL6 for more than 8 generations. All animals were housed in the animal care unit of the Washington University School of Medicine and were maintained according to guidelines of the Association for Assessment and Accreditation of Laboratory Animal Care. All animal procedures were approved by the Animal Studies Committee of the Washington University School of Medicine.

Serum CTx-I, osteocalcin and PTH measurements

Blood was collected retro-orbitally under anesthesia immediately prior to sacrifice. Serum CTx-I, a specific marker of osteoclastic bone resorption, was measured using a RatLaps ELISA kit from Nordic Bioscience Diagnostics A/S. Serum osteocalcin levels were measured by ELISA (Biomedical Technologies Inc). Plasma was obtained using plasma separator tubes with lithium heparin (Becton Dickinson) and PTH levels were measured by ELISA (Immutopics).

Histology and Histomorphometry

The tibiae of 2-month old Syt $VII^{+/+}$ and Syt $VII^{-/-}$ mice were fixed with 70% ethanol followed by plastic embedding and Goldner staining, or with 10% neutral buffered formalin followed

by the decalcification in 14% EDTA for 4–5 days, paraffin embedding, and TRAP staining. Osteoclastic and osteoblastic perimeters were measured and analyzed using Osteomeasure (OsteoMetrics, Atlanta, GA) in a blinded fashion.

μCT

The trabecular volume in the distal femoral metaphysis was measured using a Scanco μCT40 scanner (Scanco Medical AG, Basserdorf, Switzerland). A threshold of 300 was used for evaluation of all scans. 30 slices were analyzed, starting with the first slice in which condyles and primary spongiosa were no longer visible.

Osteoclast culture and bone resorption assays

BMMs were prepared as described previously (Zhao et al., 2005) with slight modification. Whole bone marrow was extracted from tibiae and femora of 6–8 weeks old Syt $VII^{+/+}$ and Syt $VII^{-/-}$ mice and incubated in red blood cell lysis buffer (150mM NH_4Cl, 10mM $KNCO_3$, 0.1mM EDTA, pH 7.4) for 5 minutes. The cells were then cultured in α10 medium (α-MEM, 10% heat-inactivated fetal bovine serum, 100IU/ml penicillin and 100μg/ml streptomycin) with 1/10 vol of CMG 14–12 culture supernatant (Takeshita et al., 2000). Osteoclasts were generated after five days culture of BMMs with 1/100 vol of CMG 14–12 culture supernatant and 100 ng/ml of recombinant RANKL. The cells cultured on plastic dishes were fixed with 4% paraformaldehyde/PBS and TRAP was stained with a commercial kit (387-A, Sigma). The staining of resorption lacunae was performed as described previously. Briefly, osteoclasts were removed by wiping the surface of bone slices with a soft brush. The slices were incubated with 20μg/ml peroxidase-conjugated wheat germ agglutinin for 30 minutes. After washing in PBS, 0.52 mg/ml 3,3'-diaminobenzidine was added onto the slices for 30 minutes. Photographs were taken under a conventional microscope equipped with a CCD camera (Nikon USA).

Osteoblast culture and bone formation assays

Primary osteoblasts were harvested from the calvariae of 3–5 day-old mice by serial collagenase digestion and cultured for 21 days with differentiation media containing 50 μg/ml ascorbic acid and 2mM β-glycerophosphate. Cells were fixed in 4% paraformaldehyde/PBS and alkaline phosphatase was stained with a kit (85L2, Sigma-Aldrich). Bone nodules were stained with Alizarin Red.

Intra- and extra-cellular collagen determination

Collagen levels were determined as described previously (Batemen and Golub, 1994). Briefly, osteoblasts cultured in a 100mm dish were harvested in lysis buffer containing 50mM Tris HCl, pH 7.4, 150mM NaCl and Halt™ proteinase inhibitor cocktail (Pierce). The cells were disrupted by sonication and extracted on ice for 30 minutes. The lysates were spun at maximum speed in a microcentrifuge for 30 minutes at 4°C. The supernatant of the cell lysates was saved for western blot analysis. 200 μl of 0.5M acetic acid was added to the cell pellet and incubated overnight at 4°C. After centrifugation, the acetic acid insoluble residue was then digested with pepsin (0.1 μg/ml, Sigma) in 200 μl of 0.5 M acetic acid at 4°C for 2 days. The supernatant of the pepsin digest extract was lyophilized and the digest residue dissolved in SDS sample buffer followed by western blot analysis for type I collagen.

Immunofluorescence

Cells were first fixed with 4% paraformaldehyde in PBS for 20 minutes. Free aldehyde groups were quenched with 50 mM NH_4Cl in PBS for 10 minutes, followed by permeabilization and blocking in PBS/0.2% BSA/0.1% saponin (PBSBS) for 30 minutes. Specific proteins were labeled with primary and secondary antibodies in PBSBS for 45 minutes. F-actin was stained

with Alexa488-phalloidin. Samples were mounted with 90% glycerol/PBS and observed using a conventional microscope equipped with a CCD camera (Nikon USA) or a confocal laser scanning microscope (LSM, Zeiss) (Zhao et al., 2002).

Electron microscopy

The tibiae of 2-month old Syt VII$^{+/+}$ and Syt VII$^{-/-}$ mice were fixed with 5% glutaraldehyde in 0.16 M collidine buffer (pH 7.4) overnight and then decalcified in 5% EDTA/0.1% glutaraldehyde for 7 days. The samples were then post-fixed in 2% OsO4/3% K-ferrocyanide for 2 hours, dehydrated in ethanol and embedded in Epon LX 112. Ultra-thin sections were stained briefly with lead citrate and examined using a JEOL 100SX transmission electron microscope.

Ultracentrifugation and fractionation

Mature osteoclasts were harvested in homogenization buffer containing 10mM HEPES, pH7.4, 250mM sucrose, 1mM EDTA plus protease inhibitors. Cells were disrupted by 10 passages through a 25-gauge needle followed by 20 strokes in a Dounce homogenizer. Nuclei and unbroken cells were pelleted by centrifugation at 1000g for 10 minutes. The post-nuclear supernatant was mixed with 50% iodixanol working solution (diluted from OptiPrep™, purchased from Greiner Bio-one) to make a 17.5% iodixanol final concentration (Gille and Nohl, 2000; Graham et al., 1994). The mixture was spun for 3 hours at 350,000g in a VTi80 rotor (Beckman). 0.2ml fractions were collected from the bottom of the tube. The density of each fraction was measured by a refractometer (Fisher).

RT-PCR

Total RNA was purified from different stages of osteoclast and osteoblast cultures by using the RNeasy Mini Kit (Qiagen). cDNAs were synthesized from 1μg of total RNA using the SuperScript First-Strand Synthesis System (Invitrogen) in a volume of 20 μl. The reaction mixture was adjusted to 100 μl with dH_2O for PCR analysis. 1 μl of these cDNAs were then amplified with primers specific for β3 integrin (sense, 5′-TTACCCCGTGGACATCTACTA-3′; antisense, 5′-AGTCTTCCATCCAGGGCAATA-3′), cathepsin K (sense, 5′-GGAAGAAGACTCACCAGAAGC-3′; antisense, 5′-GTCATATAGCCGCCTCCACAG-3′), MMP-9 (sense, 5′-CCTGTGTGTTCCCGTTCATCT-3′; antisense, 5′-CGCTGGAATGATCTAAGCCCA-3′), ALP (sense, 5′-CCCTGAAACTCCAAAAGCTC-3′; antisense, 5′-TCTGGTGGCATCTCGTTATC-3′), osteocalcin (sense, 5′-TCTGACAAAGCCTTCATGTCC-3′; antisense, 5′-AAATAGTGATACCGTAGATGCG-3′) and GAPDH (sense, 5′-ACTTTGTCAAGCTCATTTCC-3′; antisense, 5′-TGCAGCGAACTTTATTGATG-3′). After 20–35 cycles of 94°C (30s), 60°C (30s), and 72°C (30s), 10 μl of PCR products were separated on a 1.5% agarose gel containing 0.5 μg/ml ethidium bromide.

Western Blot Analysis and Immunoprecipitation

Cultured cells were washed with ice-cold PBS and lysed in 1x RIPA buffer (Upstate). After incubation on ice for 30 min., lysates were clarified by centrifugation at 15,000 rpm for 15 min. 30–50 μg of protein was subjected to SDS-polyacrylamide gels and transferred electrophoretically onto nitrocellulose membranes by a semi-dry system (Biorad). Filters were blocked in 0.1% casein/PBS for 1 hour and incubated with primary antibodies at 4°C overnight followed by probing with fluorescent-labeled secondary antibodies. Proteins were visualized using Odyssey (LI-COR Biosciences) at the appropriate wavelength.

For immunoprecipitation, cells were washed in cold PBS and lysed on ice in buffer (20mM Hepes, pH 7.4, 120mM NaCl, 5% glycerol, 1mM DTT, 0.1% NP-40, 2mM $CaCl_2$, and protease inhibitors). Lysates were passed through a 25G needle 10 times and incubated on ice for 30 minutes and then clarified by centrifugation at 15,000 rpm for 15 minutes. One mg of protein was incubated with 5–10 μg of antibodies overnight with rotation. Protein A/G agarose was then added and incubated with rotation for 3 hours at 4°C. Immunoprecipitates were washed 4 times in lysis buffer and solubilized proteins were separated by SDS-polyacrylamide gels.

Retroviral production and macrophage/osteoblast transduction

GFP-Syt VII was cloned into the pMX-IRES-puro retroviral vector (Takeshita et al., 2007) and transfected transiently into Plat-E packing cells using FuGENE 6 transfection reagent (Roche). Virus was collected 48 hours after transfection. BMMs or neonatal osteoblasts were transduced with virus for 24 hours in the presence of M-CSF and 4μg/ml Polybrene. Cells were then selected in 4μg/ml puromycin for 3–5 days.

Supplementary Material

Refer to Web version on PubMed Central for supplementary material.

ACKNOWLEDGMENTS

Dr. T Galli (Institut National de la Sante et de la Recherche Medicale Avenir team, Paris, France) is acknowledged for providing anti-TI-VAMP antibody. We thank Paulette Shubert for editorial assistance, Monica Croke for help with q-PCR and Michael Brodt for his assistance with analysis of the bone phenotype. This work was funded by grants from the National Institutes of Health, AR046852, AR054190 (FPR), AR032788, AR046523 (SLT).

REFERENCES

Anderson HC. Molecular biology of matrix vesicles. Clin Orthop 1995;314:266–280. [PubMed: 7634645]

Anderson HC, Garimella R, Tague SE. The role of matrix vesicles in growth plate development and biomineralization. Front Biosci 2005;10:822–837. [PubMed: 15569622]

Andrews NW, Chakrabarti S. There's more to life than neurotransmission: the regulation of exocytosis by synaptotagmin VII. Trends Cell Biol 2005;15:626–631. [PubMed: 16168654]

Arantes RM, Andrews NW. A role for synaptotagmin VII-regulated exocytosis of lysosomes in neurite outgrowth from primary sympathetic neurons. J Neurosci 2006;26:4630–4637. [PubMed: 16641243]

Baron R, Neff L, Brown W, Courtoy PJ, Louvard D, Farquhar M. Polarized secretion of lysosomal enzymes: Co-distribution of cation-independent mannose-6-phosphate receptors and lysosomal enzymes along the osteoclast exocytic pathway. J Cell Biol 1988;106:1863–1872. [PubMed: 2968345]

Batemen JF, Golub SB. Deposition and selective degradation of structurally-abnormal type I collagen in a collagen matrix produced by osteogenesis imperfecta fibroblasts in vitro. Matrix Biol 1994;14:251–262. [PubMed: 7921542]

Boyd C, Hughes T, Pypaert M, Novick P. Vesicles carry most exocyst subunits to exocytic sites marked by the remaining two subunits, Sec3p and Exo70p. J Cell Biol 2004;167:889–901. [PubMed: 15583031]

Chakrabarti S, Kobayashi KS, Flavell RA, Marks CB, Miyake K, Liston DR, Fowler KT, Gorelick FS, Andrews NW. Impaired membrane resealing and autoimmune myositis in synaptotagmin VII-deficient mice. J Cell Biol 2003;162:543–549. [PubMed: 12925704]

Chalhoub N, Benachenhou N, Rajapurohitam V, Pata M, Ferron M, Frattini A, Villa A, Vacher J. Grey-lethal mutation induces severe malignant autosomal recessive osteopetrosis in mouse and human. Nat Med 2003;9:399–406. [PubMed: 12627228]

Chapman ER. Synaptotagmin: a Ca2+ sensor that triggers exocytosis? Nature Reviews Molecular Cell Biology 2002;3:498–508.

Chieregatti E, Meldolesi J. Regulated exocytosis: new organelles for nonsecretory purposes. Nat Rev Mol Cell Biol 2005;6:181–187. [PubMed: 15688003]

Czibener C, Sherer NM, Becker SM, Pypaert M, Hui E, Chapman ER, Mothes W, Andrews NW. Ca2+ and synaptotagmin VII-dependent delivery of lysosomal membrane to nascent phagosomes. J Cell Biol 2006;174:997–1007. [PubMed: 16982801]

Drake FH, Dodds RA, James IE, Connor JR, Debouck C, Richardson S, Leerykaczewski E, Coleman L, Rieman D, Barthlow R, et al. Cathepsin K, but not Cathepsins B, L, or S, is abundantly expressed in human osteoclasts. J Biol Chem 1996;271:12511–12516. [PubMed: 8647859]

Ducy P, Schinke T, Karsenty G. The osteoblast: a sophisticated fibroblast under central surveillance. Science 2000;289:1501–1504. [PubMed: 10968779]

Feng X, Novack DV, Faccio R, Ory DS, Aya K, Boyer MI, McHugh KP, Ross FP, Teitelbaum SL. A Glanzmann's mutation in β3 integrin specifically impairs osteoclast function. J Clin Invest 2001;107:1137–1144. [PubMed: 11342577]

Fowler KT, Andrews NW, Huleatt JW. Expression and function of synaptotagmin VII in CTLs. J Immunol 2007;178:1498–1504. [PubMed: 17237398]

Frattini A, Orchard PJ, Sobacchi C, Giliani S, Abinun M, Mattsson JP, Keeling DJ, Andersson AK, Wallbrandt P, Zecca L, et al. Defects in TCIRG1 subunit of the vacuolar proton pump are responsible for a subset of human autosomal recessive osteopetrosis. Nat Genet 2000;25:343–346. [PubMed: 10888887]

Gao Z, Reavey-Cantwell J, Young RA, Jegier P, Wolf BA. Synaptotagmin III/VII Isoforms Mediate Ca2+-induced Insulin Secretion in Pancreatic Islet beta -Cells. J Biol Chem 2000;275:36079–36085. [PubMed: 10938083]

Garimella R, Sipe JB, Anderson HC. A simple and non-radioactive technique to study the effect of monophosphoesters on matrix vesicle-mediated calcification. Biol Proced Online 2004;6:263–267. [PubMed: 15605107]

Gauthier BR, Duhamel DL, Iezzi M, Theander S, Saltel F, Fukuda M, Wehrle-Haller B, Wollheim CB. Synaptotagmin VII splice variants α, β, and γ are expressed in pancreatic β-cells and regulate insulin exocytosis. FASEB J. 2007E Pub Ahead of Print.

Gelb BD, Shi GP, Chapman HA, Desnick RJ. Pycnodysostosis, a lysosomal disease caused by cathepsin K deficiency. Science 1996;273:1236–1238. [PubMed: 8703060]

Genge BR, Wu LN, Wuthier RE. Separation and quantification of chicken and bovine growth plate cartilage matrix vesicle lipids by high-performance liquid chromatography using evaporative light scattering detection. Anal Biochem 2003;322:104–115. [PubMed: 14705786]

Geppert M, Goda Y, Hammer RE, Li C, Rosahi TW, Stevens CF, Sudhof TC. Synaptotagmin I: A major Ca 2+ sensor for transmitter release at a central synapse. Cell 1994;79:717–727. [PubMed: 7954835]

Gille L, Nohl H. The existence of a lysosomal redox chain and the role of ubiquinone. Arch Biochem Biophys 2000;375:347–354. [PubMed: 10700391]

Gorski JP, Huffman NT, Wright H. Proteomic analysis of bone biomineralization foci isolated by laser capture microscopy from osteoblast cultures. J Bone Miner Res 2005;20:S109.

Graham J, Ford T, Rickwood D. The preparation of subcellular organelles from mouse liver in self-generated gradients of iodixanol. Anal Biochem 1994;220:367–373. [PubMed: 7978280]

Hammarlund M, Watanabe S, Schuske K, Jorgensen EM. CAPS and syntaxin dock dense core vesicles to the plasma membrane in neurons. J Cell Biol. 2008E Pub Ahead of Print.

Harada S, Rodan GA. Control of osteoblast function and regulation of bone mass. Nature 2003;423:349–355. [PubMed: 12748654]

Jahn R, Scheller RH. SNAREs--engines for membrane fusion. Nat Rev Mol Cell Biol 2006;7:631–643. [PubMed: 16912714]

Kawamura N, Kugimiya F, Oshima Y, Ohba S, Ikeda T, Saito T, Shinoda Y, Kawasaki Y, Ogata N, Hoshi K, et al. Akt1 in osteoblasts and osteoclasts controls bone remodeling. PLoS ONE 2007;2:e1058. [PubMed: 17957242]

Kirsch T, Nah HD, Shapiro IM, Pacifici M. Regulated production of mineralization-competent matrix vesicles in hypertrophic chondrocytes. J Cell Biol 1997;137:1149–1160. [PubMed: 9166414]

Kornak U, Kasper D, Bosl MR, Kaiser E, Schweizer M, Schulz A, Friedrich W, Delling G, Jentsch TJ. Loss of the ClC-7 chloride channel leads to osteopetrosis in mice and man. Cell 2001;104:205–215. [PubMed: 11207362]

Lange PF, Wartosch L, Jentsch TJ, Fuhrmann JC. ClC-7 requires Ostm1 as a beta-subunit to support bone resorption and lysosomal function. Nature 2006;440:220–223. [PubMed: 16525474]

Li Y, Wang P, Xu J, Gorelick F, Yamazaki H, Andrews N, Desir GV. Regulation of insulin secretion and GLUT4 trafficking by the calcium sensor synaptotagmin VII. Biochem Biophys Res Commun. 2007E Pub Ahead of Print.

Li YP, Chen W, Liang Y, Li E, Stashenko P. Atp6i-deficient mice exhibit severe osteopetrosis due to loss of osteoclast-mediated extracellular acidification. Nat Genet 1999;23:447–451. [PubMed: 10581033]

Martinez I, Chakrabarti S, Hellevik T, Morehead J, Fowler K, Andrews NW. Synaptotagmin VII Regulates Ca2+-dependent Exocytosis of Lysosomes in Fibroblasts. J Cell Biol 2000;148:1141–1150. [PubMed: 10725327]

Meldolesi J, Chieregatti E. Fusion has found its calcium sensor. Nat Cell Biol 2004;6:476–478. [PubMed: 15170455]

Osborne SL, Wallis TP, Jimenez JL, Gorman JJ, Meunier FA. Identification of secretory granule phosphatidylinositol 4,5-bisphosphate-interacting proteins using an affinity pulldown strategy. Mol Cell Proteomics 2007;6:1158–1169. [PubMed: 17449848]

Prele CM, Horton MA, Caterina P, Stenbeck G. Identification of the molecular mechanisms contributing to polarized trafficking in osteoblasts. Exp Cell Res 2003;282:24–34. [PubMed: 12490191]

Prockop DJ, Kivirikko KI. Collagens: molecular biology, diseases, and potentials for therapy. Annu Rev Biochem 1995;64:403–434. [PubMed: 7574488]

Raisz LG. Pathogenesis of osteoporosis: concepts, conflicts, and prospects. J Clin Invest 2005;115:3318–3325. [PubMed: 16322775]

Rao SK, Huynh C, Proux-Gillardeaux V, Galli T, Andrews NW. Identification of SNAREs Involved in Synaptotagmin VII-regulated Lysosomal Exocytosis. J Biol Chem 2004;279:20471–20479. [PubMed: 14993220]

Reddy A, Caler EV, Andrews NW. Plasma Membrane Repair Is Mediated by Ca2+-Regulated Exocytosis of Lysosomes. Cell 2001;106:157–169. [PubMed: 11511344]

Rizo J, Chen X, Arac D. Unraveling the mechanisms of synaptotagmin and SNARE function in neurotransmitter release. Trends Cell Biol 2006;16:339–350. [PubMed: 16698267]

Rizo J, Sudhof TC. C2-domains, Structure and Function of a Universal Ca2+-binding Domain. J Biol Chem 1998;273:15879–15882. [PubMed: 9632630]

Roberts S, Narisawa S, Harmey D, Millán JL, Farquharson C. Functional Involvement of PHOSPHO1 in Matrix Vesicle Mediated Skeletal Mineralization. J Bone Miner Res 2007;22:617–627. [PubMed: 17227223]

Saftig P, Hunziker E, Wehmeyer O, Jones S, Boyde A, Rommerskirch W, Moritz JD, Schu P, von Figura K. Impaired osteoclastic bone resorption leads to osteopetrosis in cathepsin-K-deficient mice. Proc Natl Acad Sci U S A 1998;95:13453–13458. [PubMed: 9811821]

Saita Y, Takagi T, Kitahara K, Usui M, Miyazono K, Ezura Y, Nakashima K, Kurosawa H, Ishii S, Noda M. Lack of Schnurri-2 expression associates with reduced bone remodeling and osteopenia. J Biol Chem 2007;282:12907–12915. [PubMed: 17311925]

Schroder B, Wrocklage C, Pan C, Jager R, Kosters B, Schafer H, Elsasser HP, Mann M, Hasilik A. Integral and associated lysosomal membrane proteins. Traffic 2007;8:1676–1686. [PubMed: 17897319]

Shao JS, Cai J, Towler DA. Molecular mechanisms of vascular calcification: lessons learned from the aorta. Arterioscler Thromb Vasc Biol 2006;26:1423–1430. [PubMed: 16601233]

Silva MJ, Brodt MD, Uthgenannt BA. Morphological and mechanical properties of caudal vertebrae in the SAMP6 mouse model of senile osteoporosis. Bone 2004;35:425–431. [PubMed: 15268893]

Sudhof TC, Rizo J. Synaptotagmins: C2-domain proteins that regulate membrane traffic. Neuron 1996;17:379–388. [PubMed: 8816702]

Sugita S, Shin O-H, Han W, Lao Y, Sudhof TC. Synaptotagmins form a hierarchy of exocytotic Ca2+ sensors with distinct Ca2+ affinities. EMBO J 2002;21:270–280. [PubMed: 11823420]

Takano Y, Sakai H, Baba O, Terashima T. Differential involvement of matrix vesicles during the initial and appositional mineralization processes in bone, dentin, and cementum. Bone 2000;26:333–339. [PubMed: 10719275]

Takayanagi H, Kim S, Koga T, Nishina H, Isshiki M, Yoshida H, Saiura A, Isobe M, Yokochi T, Inoue J, et al. Induction and activation of the transcription factor NFATc1 (NFAT2) integrate RANKL signaling in terminal differentiation of osteoclasts. Dev Cell 2002;3:889–901. [PubMed: 12479813]

Takeshita S, Faccio R, Chappel JC, Zheng L, Feng S, Weber JD, Teitelbaum SL, Ross FP. c-Fms tyrosine 559 Is a major mediator of M-CSF-induced proliferation of primary macrophages. J Biol Chem 2007;282:18980–18990. [PubMed: 17420255]

Takeshita S, Kaji K, Kudo A. Identification and characterization of the new osteoclast progenitor with macrophage phenotypes being able to differentiate into mature osteoclasts. J Bone Miner Res 2000;15:1477–1488. [PubMed: 10934646]

Teitelbaum SL, Ross FP. Genetic regulation of osteoclast development and function. Nat Rev Genet 2003;4:638–649. [PubMed: 12897775]

TerBush DR, Maurice T, Roth D, Novick P. The Exocyst is a multiprotein complex required for exocytosis in Saccharomyces cerevisiae. EMBO J 1996;15:6483–6494. [PubMed: 8978675]

Tolar J, Teitelbaum SL, Orchard PJ. Osteopetrosis. N Engl J Med 2004;351:2839–2849. [PubMed: 15625335]

Toyomura T, Murata Y, Yamamoto A, Oka T, Sun-Wada G-H, Wada Y, Futai M. From Lysosomes to the Plasma Membrane: LOCALIZATION OF VACUOLAR TYPE H+-ATPase WITH THE a3 ISOFORM DURING OSTEOCLAST DIFFERENTIATION. J Biol Chem 2003;278:22023–22030. [PubMed: 12672822]

Tsuboi T, Fukuda M. Synaptotagmin VII modulates the kinetics of dense-core vesicle exocytosis in PC12 cells. Genes Cells 2007;12:511–519. [PubMed: 17397398]

Vaananen HK, Zhao H, Mulari M, Halleen JM. The cell biology of osteoclast function. J Cell Sci 2000;113:377–381. [PubMed: 10639325]

Verhage M, Toonen RF. Regulated exocytosis: merging ideas on fusing membranes. Curr Opin Cell Biol 2007;19:402–408. [PubMed: 17629692]

Wang P, Chicka MC, Bhalla A, Richards DA, Chapman ER. Synaptotagmin VII is targeted to secretory organelles in PC12 cells, where it functions as a high-affinity calcium sensor. Mol Cell Biol 2005;25:8693–8702. [PubMed: 16166648]

Wiesmann HP, Meyer U, Plate U, Hohling HJ. Aspects of collagen mineralization in hard tissue formation. Int Rev Cytol 2005;242:121–156. [PubMed: 15598468]

Winslow MM, Pan M, Starbuck M, Gallo EM, Deng L, Karsenty G, Crabtree GR. Calcineurin/NFAT signaling in osteoblasts regulates bone mass. Dev Cell 2006;10:771–782. [PubMed: 16740479]

Xiao Z, Awad HA, Liu S, Mahlios J, Zhang S, Guilak F, Mayo MS, Quarles LD. Selective Runx2-II deficiency leads to low-turnover osteopenia in adult mice. Dev Biol 2005;283:345–356. [PubMed: 15936013]

Xiao Z, Camalier CE, Nagashima K, Chan KC, Lucas DA, de la Cruz MJ, Gignac M, Lockett S, Issaq HJ, Veenstra TD, et al. Analysis of the extracellular matrix vesicle proteome in mineralizing osteoblasts. J Cell Physiol 2007;210:325–335. [PubMed: 17096383]

Zaidi M. Skeletal remodeling in health and disease. Nat Med 2007;13:791–801. [PubMed: 17618270]

Zhao H, Ettala O, Vaananen HK. Intracellular membrane trafficking pathways in bone-resorbing osteoclasts revealed by cloning and subcellular localization studies of small GTP-binding rab proteins. Biochem Biophys Res Commun 2002;293:1060–1065. [PubMed: 12051767]

Zhao H, Kitaura H, Sands MS, Ross FP, Teitelbaum SL, Novack DV. Critical role of β3 integrin in experimental postmenopausal osteoporosis. J Bone Miner Res 2005;20:2116–2123. [PubMed: 16294265]

Zhao H, Laitala-Leinonen T, Parikka V, Vaananen HK. Downregulation of small GTPase Rab7 impairs osteoclast polarization and bone resorption. J Biol Chem 2001;276:39295–39302. [PubMed: 11514537]

Zhao H, Vaananen HK. Pharmacological sequestration of intracellular cholesterol in late endosomes disrupts ruffled border formation in osteoclasts. J Bone Miner Res 2006;21:456–465. [PubMed: 16491294]

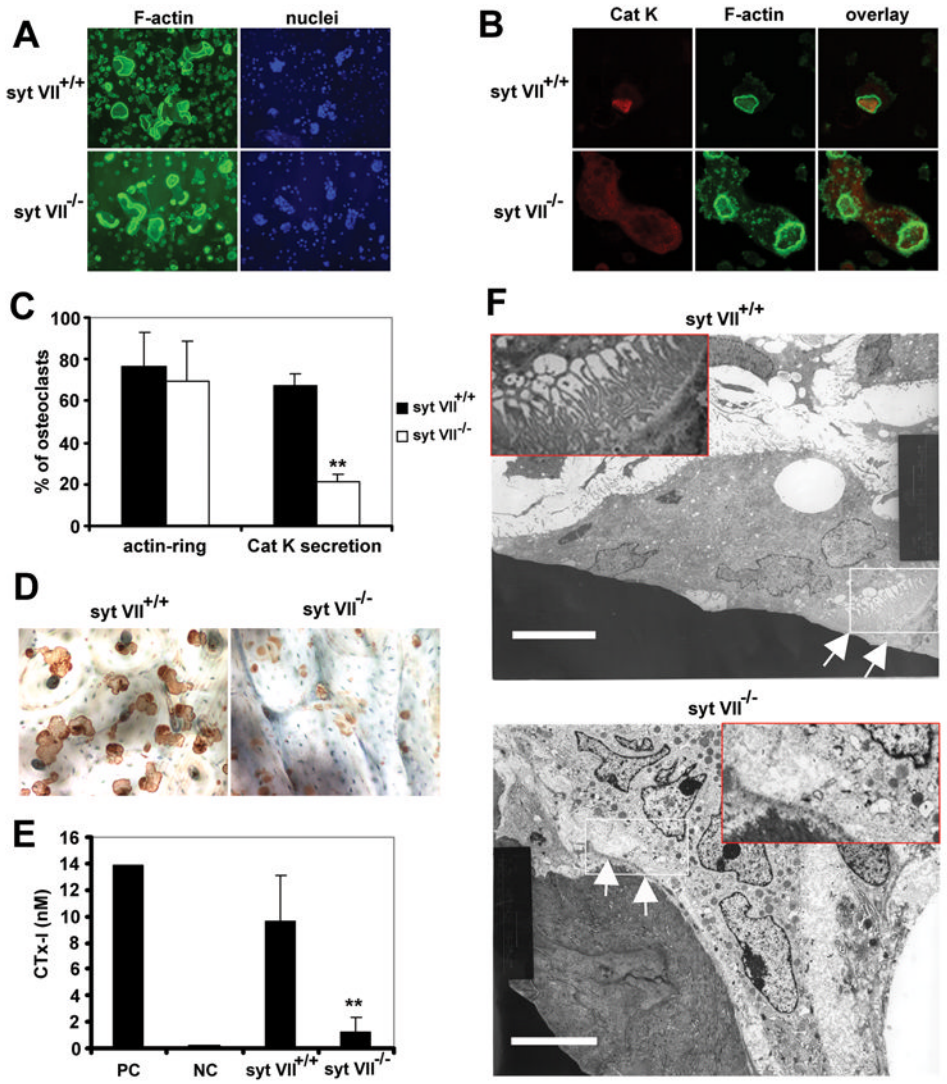

Figure 1. Syt VII$^{-/-}$ osteoclasts have defects in cathepsin K secretion and ruffled border formation

(A) Syt VII$^{+/+}$ and Syt VII$^{-/-}$ BMMs were cultured with M-CSF and RANKL on bone slices for 5 days. F-actin and nuclei were stained with Alexa-488 phalloidin and Hoechst 33258 respectively. **(B)** Cathepsin K (Cat K) was co-stained with F-actin. The secretion of Cat K into the resorption lacunae, which are circumscribed by actin-rings, was detected by confocal microscopy. **(C)** Total and cathepsin K-containing cells in **(A)** and **(B)** were counted. Data are presented as mean ± SD n=5 in each group. ** p< 0.01 versus WT. **(D)** Osteoclasts were removed from bone slices and resorption pits were labeled with peroxidase-conjugated wheat germ agglutinin. **(E)** Medium CTx-I level was measured by ELISA. Lane 1, positive control in the kit; lane 2, medium alone control; lane 3, Syt VII$^{+/+}$ cultures; lane 4, Syt VII$^{-/-}$. Data are presented as mean ± SD n=6 in each group. ** p< 0.01 versus WT. **(F)** Transmission electron microscopic images. White arrows and an enlarged insert in the upper panel identify the convoluted ruffled border in a Syt VII$^{+/+}$ osteoclast. This membrane structure is not observed in a Syt VII$^{-/-}$ osteoclast (white arrows and an enlarged insertion in the lower panel). White rectangles show the area enlarged in the inserts. Scale bars = 6.8 μm.

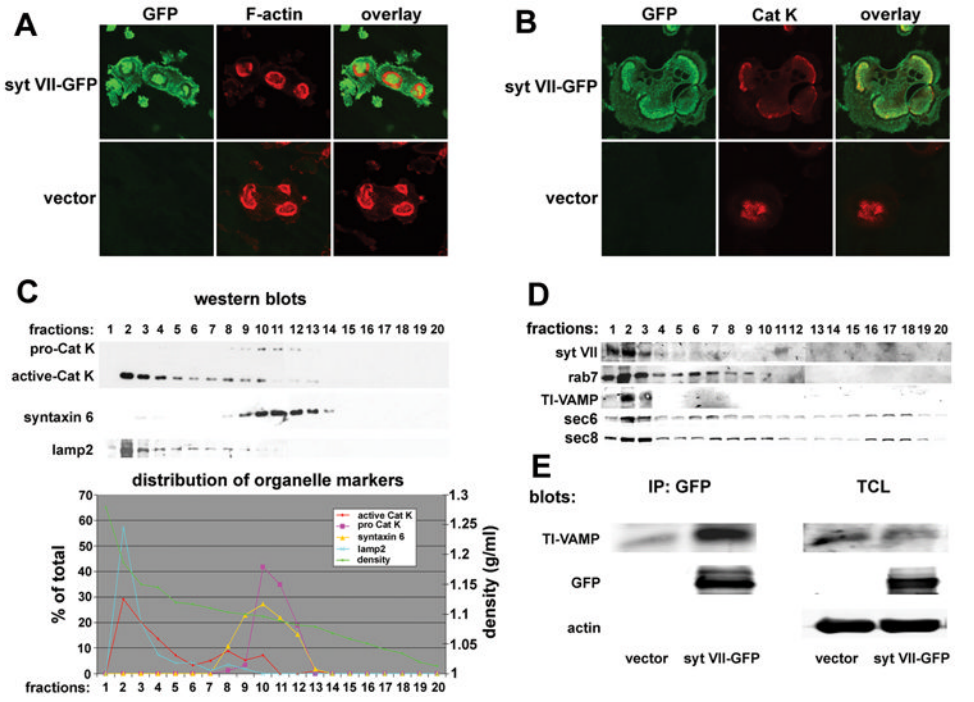

Figure 2. Syt VII associates with lysosomes in osteoclasts and translocates to the ruffled border

(A) and **(B)** BMMs transduced with Syt VII-GFP were cultured with MCSF and RANKL on bone slices for 5 days. Syt VII-GFP was co-stained for F-actin (A) or cathepsin K (Cat K). Cells transduced with empty vector served as staining controls. **(C)** and **(D)** Cytosol of mature osteoclasts was fractionated by iodixanol ultracentrifugation. The distribution of Syt VII, lysosomal proteins and organelle markers was detected by western blots and the data displayed graphically. **(E)** Syt VII immunoprecipitates were assessed for the presence of the lysosomal v-SNARE TI-VAMP. TCL, 5% of total cell lysates.

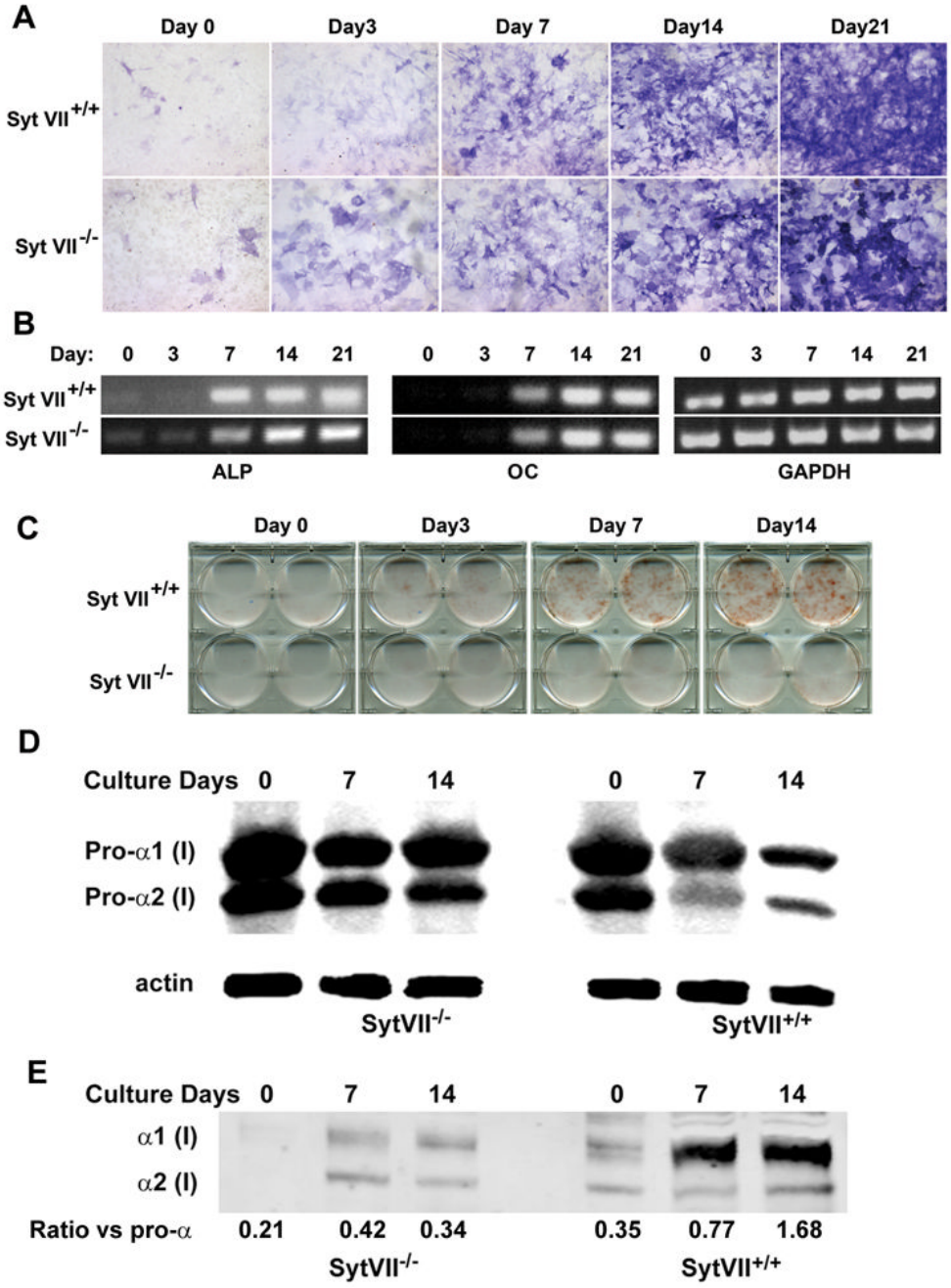

Figure 3. Syt VII$^{-/-}$ osteoblasts differentiate normally but form fewer bone nodules

(A) Syt VII$^{+/+}$ and Syt VII$^{-/-}$ primary calvarial osteoblasts were cultured with differentiation media containing 50 μg/ml ascorbic acid and 2 mM β-glycerophosphate for 21 days. Cells were fixed at different days and stained for alkaline phosphatase (ALP). **(B)** Expression of ALP and osteocalcin (OC) mRNA was analyzed by RT-PCR. GAPDH served as loading control. **(C)** Bone nodule formation was visualized with time by Alizarin Red staining. **(D)** The intracellular pro-alpha chains of type I collagen in total cell lysates were detected by western blot. Actin served as loading control. **(E)** The extracellular mature form of type I collagen alpha chains in pepsin-digested extracts was detected by western blot with the same

antibody as in **(D)**. The density of α1 bands in **(D)** and **(E)** was quantified using NIH Image J programme and expressed as a ratio.

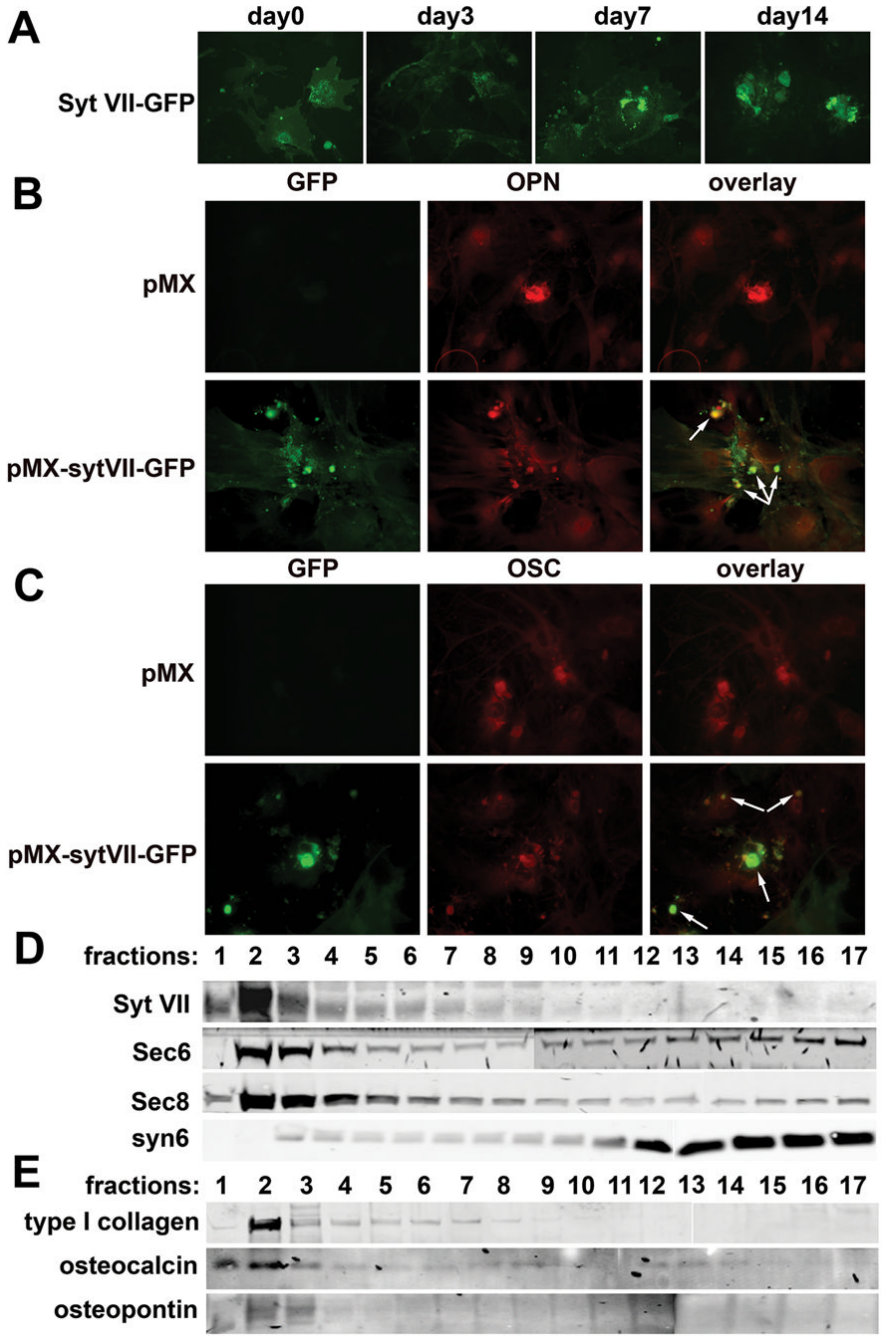

Figure 4. Syt VII associates with bone matrix proteins in osteoblasts

(A) The localization of Syt VII-GFP was visualized at different days of osteoblast differentiation cultures under fluorescent microscopy. **(B)** and **(C)** Syt VII-GFP was co-stained with osteopontin (OPN) or osteocalcin (OC) in day 14 osteoblast cultures by fluorescent microscopy. Empty vector transduced cells served as staining controls. Arrows in **(B)** and **(C)** overlays indicate co-localization of Syt VII with OPN and OC, respectively. **(D)** and **(E)** The cytosol of day 14 cultured osteoblasts was fractionated by iodixanol ultracentrifugation. The distribution of Syt VII, organelle markers and bone matrix proteins was detected by western blot analysis.

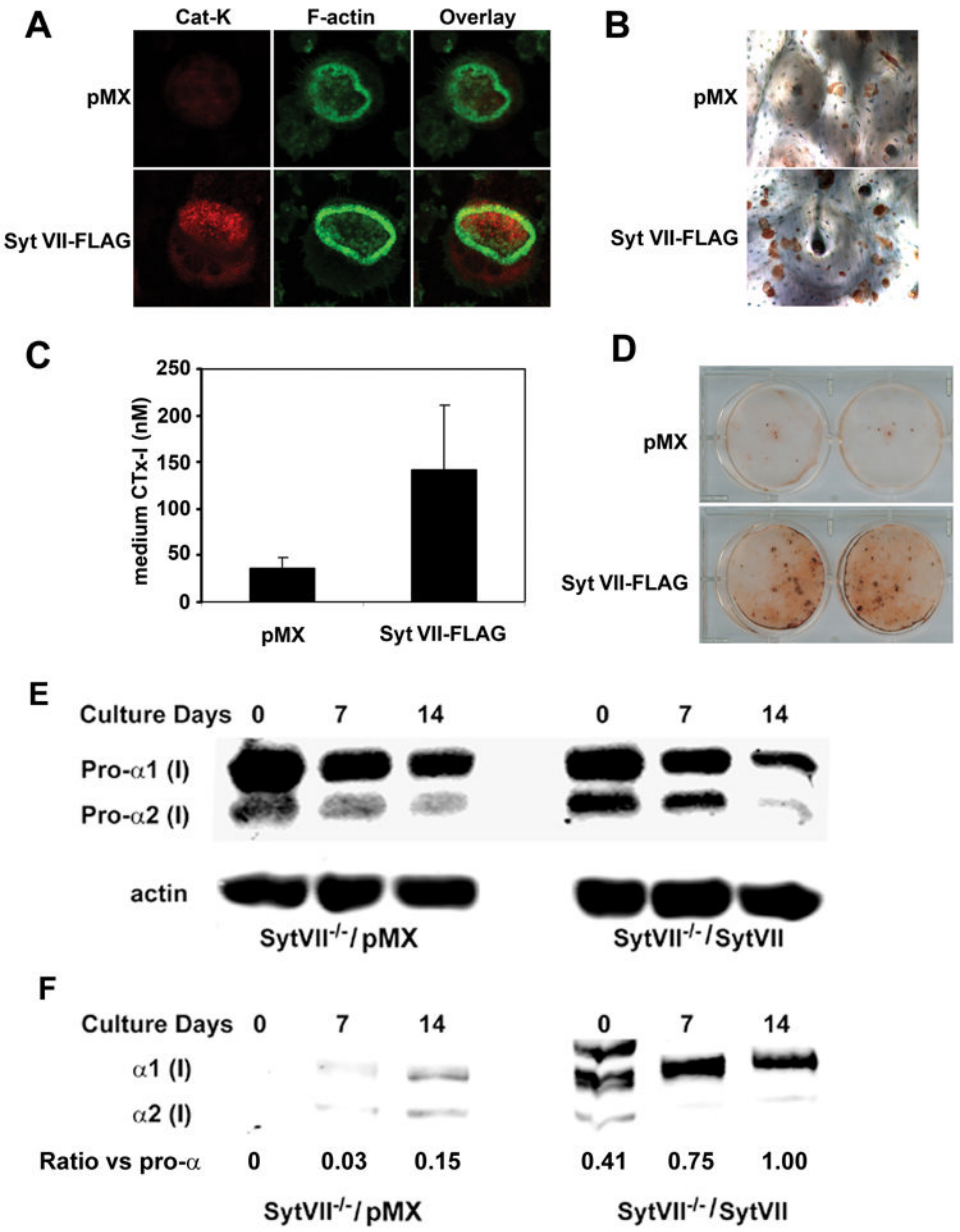

Figure 5. Retroviral transduction of WT Syt VII reconstitutes the function of Syt VII$^{-/-}$ osteoclasts and osteoblasts

Syt VII$^{-/-}$ BMMs and primary osteoblasts were isolated and transduced with empty vector or FLAG-tagged WT Syt VII. Transduced BMMs were cultured with M-CSF and RANKL on bone slices for 5 days. Osteoblasts were cultured with differentiation media for 21 days. **(A)** co-staining of cathepsin K (Cat K) and F-actin. **(B)** Pit staining. **(C)** Medium CTx-I assay. Data are presented as mean ± SD n=6 in each group. ** $p<0.01$ versus vector pMX. **(D)** Bone nodule staining. * $p< 0.05$ versus empty vector cultures. **(E)** The level of intracellular pro-alpha chains of type I collagen in total cell lysates was detected by western blot. Actin served as loading control. **(F)** Western blot of extracellular mature form of type I collagen alpha chains in pepsin-digested extracts from Syt VII$^{-/-}$ and wild type osteoblast cultures. The density of α1 bands in **(E)** and **(F)** was measured using NIH Image J programme and expressed as a ratio.

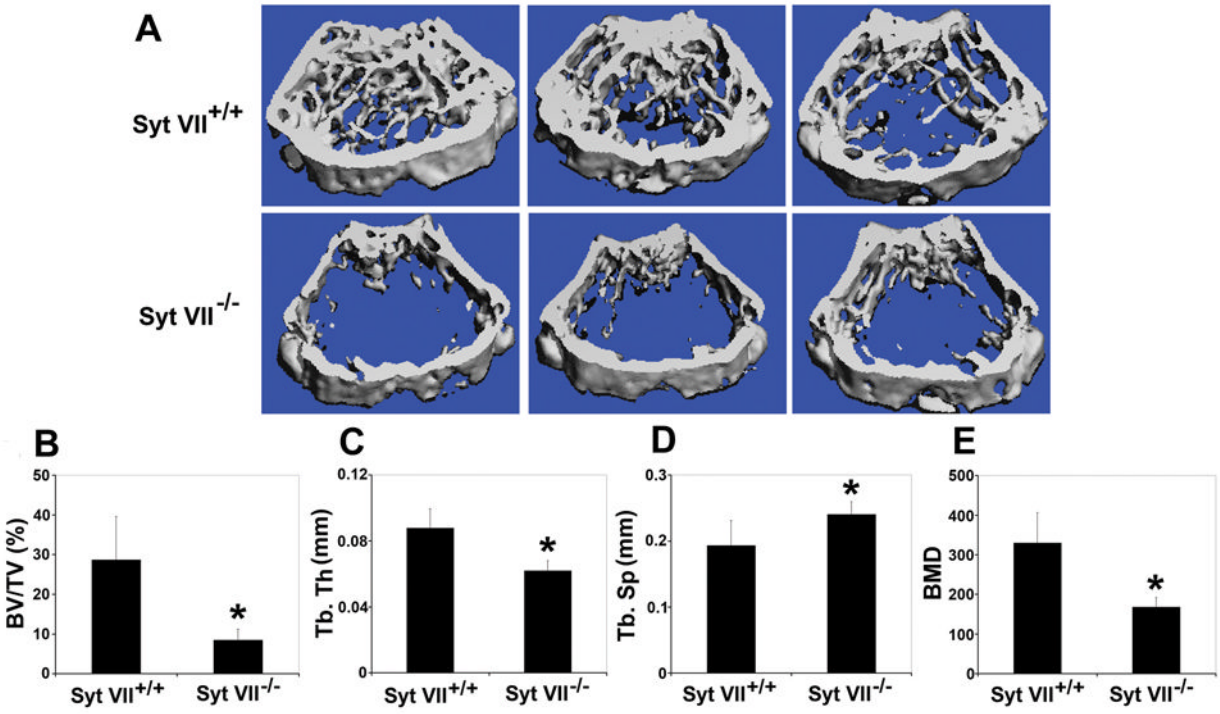

Figure 6. Syt VII$^{-/-}$ mice are osteopenic

(A) Representative 3D reconstruction of μCT images of distal femoral metaphysis from three different mice of each genotype. **(B)** The percentage of trabecular bone volume/tissue volume (BV/TV). **(C)** Trabecular thickness (Tb.Th). **(D)** Trabecular separation (Tb.Sp). **(E)** Bone mineral density (BMD). Data presented in B–E are present as mean ± SD, n=5 in each group of mice. * $p<0.05$ 40 versus WT.

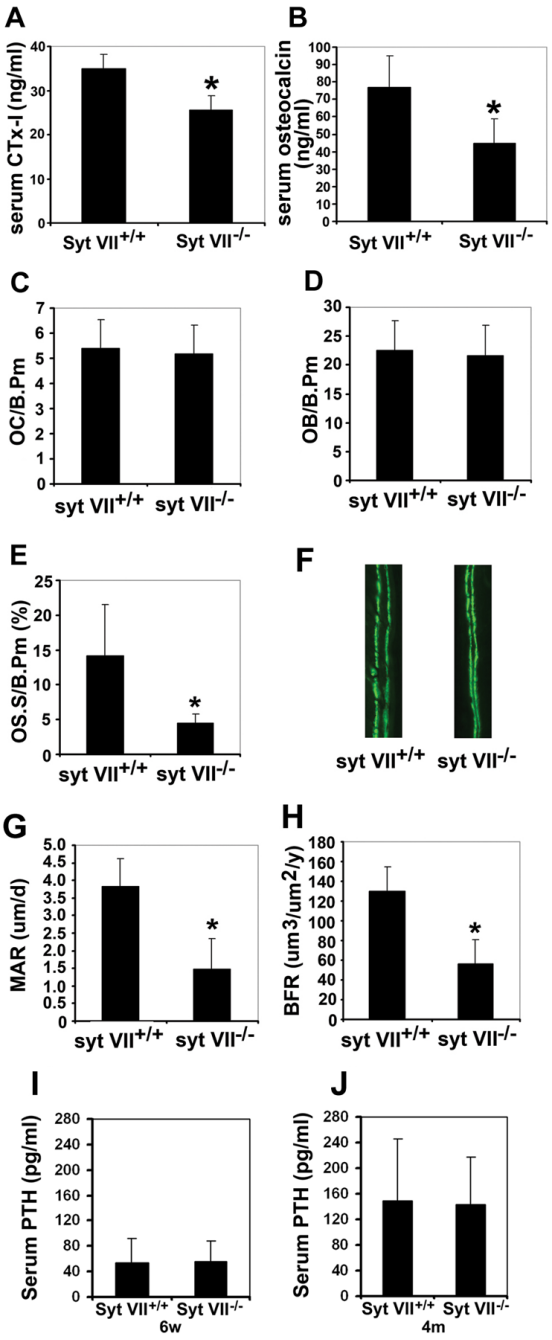

Figure 7. Decreased bone resorption and bone formation in Syt VII$^{-/-}$ mice

(A) and **(B)** Bone resorption and bone formation rates were quantified at sacrifice by serum CTx-I and osteocalcin levels, respectively. **(C)** Osteoclast number/bone perimeter (OC/B.Pm). **(D)** Osteoblast number/bone perimeter (OB/B/Pm). **(E)** Osteoid surface/bone perimeter (OS.S/B.Pm). **(F)** Representative fluorescent micrographs of calcein labeling. Data in (B) to (F) are presented as mean ± SD, n=5 in each group of mice. * $p<0.05$ versus WT. **(G)** and **(H)** Mineral apposition rate (MAR) and bone formation rate (BFR) in Syt VII$^{-/-}$ mice calculated from the data in G. Results are presented as mean ± SD, n=5 in each group of mice. * $p<0.05$ versus WT. **(I)** and **(J)** Systemic PTH levels of 6-week old (I) and 4-month old (J) wild type and Syt VII$^{-/-}$ mice. Data are presented as mean ± SD, n=4 in each group of mice.